First-principles investigation of transient spin transfer torque in magnetic multilayer systems

Zhizhou Yu,[1,2,3] Lei Zhang,[4,5,2] and Jian Wang[2,3,*]

[1]*School of Physics and Technology, Nanjing Normal University, Nanjing 210023, China*

[2]*Department of Physics and the Center of Theoretical and Computational Physics, The University of Hong Kong,*
Pokfulam Road, Hong Kong, China

[3]*The University of Hong Kong Shenzhen Institute of Research and Innovation, Shenzhen 518053, China*

[4]*State Key Laboratory of Quantum Optics and Quantum Optics Devices, Institute of Laser Spectroscopy,*
Shanxi University, Taiyuan 030006, China

[5]*Collaborative Innovation Center of Extreme Optics, Shanxi University, Taiyuan 030006, China*

By employing the nonequilibrium Green's function (NEGF) method, the transient current and the transient behavior of the spin transfer torque (STT) of the magnetic layered system are investigated within the framework of density functional theory (DFT). To reduce the huge computational cost of the transient calculation, especially when the dense mesh of k sampling is present for layered systems, the complex absorbing potential (CAP) and the Padé spectrum decomposition are used so that the energy integrals in calculating transient current and STT can be performed analytically using residue theorem, which dramatically reduces the computational complexity of the first-principles calculation of transient behavior. As an application of the NEGF-DFT-CAP formalism, the transient current and current-induced STT of the Co/Cu/Co trilayer system are studied under an upward bias pulse for different angles of magnetization direction between two leads. The transient current shows a damped oscillatory behavior with the oscillation frequency proportional to the applied bias, leading to a relaxation time of hundreds of femtoseconds. The time-dependent STTs show roughly the same profile for systems with different rotating angles. The oscillation behavior is also observed as the transient STT approaches the steady state value. Such oscillations can be attributed to the interface resonant states.

I. INTRODUCTION

The generation and manipulation of spin-polarized current have received considerable attention both experimentally and theoretically over the past decade in the magnetic multilayer structures such as the ferromagnet-normal-ferromagnet system [1,2] due to the discovery of giant magnetoresistance (GMR) [3,4] and tunnel magnetoresistance (TMR) [5,6] effect owing to their fascinating applications in information technology. By switching the magnetizations of ferromagnetic films, it was found that the electronic resistance of the parallel alignment is relatively lower than that of the antiparallel configuration originated from the dependence of electron scattering on the spin orientation. It is the basic principle of the application of magnetoresistive random-access memory, in which the magnetization direction is usually controlled by applying an external magnetic field.

Recently, the spin transfer torque (STT), proposed by Slonczewski [7] and Berger [8,9], was used to switch the magnetization orientation of the ferromagnetic layers in magnetoresistance devices. In the STT effect, a spin-polarized current can transfer the local spin angular momentum to the ferromagnetic layer. This in turn results in a torque applied to the ferromagnetic layer which can change the orientation of the magnetic layer and even flip it if the spin-polarized current is large enough. Therefore, the STT technology shows potential applications in the magnetoresistive memory with lower power consumption if the STT instead of the magnetic field is employed to control the direction of active elements in

the magnetoresistive random-access memory. Experimentally, the current-induced excitation or flip of the magnetic layer by STT has been observed in many magnetic multilayer systems such as Co/Cu multilayers [10] and Co/Cu/Co pillars [11,12].

In order to controllably use the STT effect, it is necessary to understand the current-induced torque theoretically and quantitatively. Slonczewski first presented a derivation of STT using a one-dimensional WKB approximation and only considered electrons transmitted or reflected completely by the magnetic layers [7]. A scattering formalism was then given to improve the calculation of STT in both ballistic and diffusive regimes [13]. In order to consider the nonequilibrium exchange interaction between layers, Heide *et al.* derived a set of Landau-Lifshitz equations to study the switching of magnetic layers [14,15] and an alternative mechanism of the current-induced switching was proposed from the spin accumulation due to the spin-polarized current. The Landau-Lifshitz-Gilbert equation in the presence of the dynamic STT was generalized to study various dynamic behaviors in the GMR or TMR devices [16–18].

The Landau-Lifshitz-Gilbert equation is the fundamental equation to study the dynamics of spin driven by STT caused by the imbalance of the spin current. Usually, the STT is given as a source term due to external bias or temperature gradient. Within the framework of Landau-Lifshitz-Gilbert equation, there exist two-time scales for dynamics of spin and electron responsible for STT, respectively. The fast dynamics of electron is on the order of femtosecond, while the slow dynamics of spin is on the scale of millisecond. So far the spin dynamics governed by the Landau-Lifshitz-Gilbert equation has been studied extensively, whereas the fast dynamics of STT has not been studied before. Given the fact that the concept

*jianwang@hku.hk

of STT has been used to make nonvolatile memory devices, a central question is to understand the nature of dynamics of STT, for instance, the response of STT to the external bias. Up to now, there is no microscopic theory to investigate dynamical behavior of STT. It is the purpose of this paper to address this important issue. We will ask the following question: how STT evolves with time for a sudden change of the bias in a magnetic multilayer system.

To answer this question, we will use the nonequilibrium Green's function (NEGF) formalism which has been successfully combined with the density functional theory (DFT) to study and predict the spin-polarized current and the magnetoresistance for magnetic multilayer structures in spintronics [19–24]. Recently, the steady state current-induced STT has been calculated from first principles based on the NEGF-DFT framework [21,25,26]. However, the first-principles investigation of both transient current and time-dependent STT in a magnetic multilayer system is still lacking due to its huge computational cost because a dense mesh of k points within the Brillouin zone is needed for the convergence of transmission coefficients in layered structures. For instance, 1 000 000 k points have been used to calculate the transmission coefficient of the Fe/MgO/Fe trilayer structures with $FeO_{0.5}$ buffer iron oxide layer from first principles [27]. In order to reduce the computational complexity for calculating the transient current and heat current from the exact solution within the NEGF-DFT method, the complex absorbing potential (CAP) was introduced to replace the self-energy of the lead and a linear scaling scheme was obtained for quasi-one-dimensional atomic junctions [28,29]. However, the NEGF-DFT-CAP framework has never been used for planar structures with k samplings. Moreover, in order to overcome the slow convergence for the energy integral involving the Fermi distribution functions, an efficient sum-over-poles decomposition, namely, the Padé approximation, was used to replace the Fermi functions in the time-dependent quantum transport studies [30–33].

In this paper, we developed a theoretical formalism to study the transient behavior of STT of magnetic multilayer systems under the steplike pulse of bias. In the presence of k samplings, an efficient algorithm is proposed for the first-principles calculation of transient STT within the NEGF-DFT-CAP framework and Padé approximation. As an application, we calculated both the transient current and current-induced transient STT for an upward pulse of bias in the Co/Cu/Co trilayer system from first principles.

The paper is organized as follows. In Sec. II, the formalism of transient current-induced STT in magnetic layered systems is presented under the NEGF-DFT-CAP framework with the Padé approximation. In Sec. III, the numerical calculation of both transient charge current and STT of Co/Cu/Co trilayers under an upward bias voltage is presented. Finally, the discussion and conclusion are given in Sec. IV.

II. THEORETICAL FORMALISM

The system we consider is a nonmagnetic system which connected with two semi-infinite magnetic electrodes. The magnetic moment of the left ferromagnet $\mathbf{M}_L$ is assumed to align along the in-plane y direction and the charge current
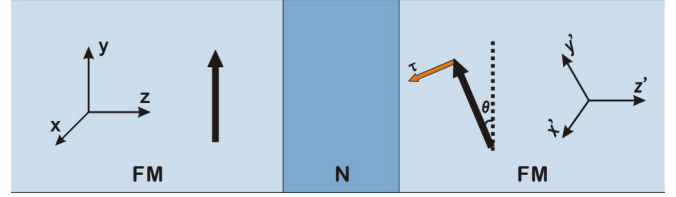

FIG. 1. Schematic illustration of the STT in the ferromagnet-normal-ferromagnet system. Electrons flow through the z direction.

flows along the z direction which is perpendicular to the layer, as shown in Fig. 1, while the magnetic moment of the right electrode $\mathbf{M}_R$ points at an angle θ to the y direction in the x-y plane of the left electrode which forms x'-y' plane in the right electrode. The Hamiltonian of the whole system can be expressed as

$$H = H_L + H_R + H_N + H_T, \tag{1}$$

where H_L and H_R are the Hamiltonian of the left and right leads, respectively,

$$H_L = \sum_{\mathbf{k}_L \sigma} [\epsilon_{\mathbf{k}_L \sigma}(t) + \sigma M_L] c_{\mathbf{k}_L \sigma}^\dagger c_{\mathbf{k}_L \sigma}, \tag{2}$$

$$H_R = \sum_{\mathbf{k}_R \sigma} [\epsilon_{\mathbf{k}_R \sigma}(t) + \sigma M_R \cos\theta] c_{\mathbf{k}_R \sigma}^\dagger c_{\mathbf{k}_R \sigma}$$

$$+ \sum_{\mathbf{k}_R \sigma} M_R \sin\theta \, c_{\mathbf{k}_R \sigma}^\dagger c_{\mathbf{k}_R \bar{\sigma}}. \tag{3}$$

Here, $c_{\mathbf{k}_\alpha \sigma}^\dagger$ ($c_{\mathbf{k}_\alpha \sigma}$) is the creation (annihilation) operator of electrons with spin σ in the α ($\alpha = L, R$) lead where $\sigma = \uparrow, \downarrow$ or ± 1 and $\bar{\sigma} = -\sigma$. $\epsilon_{\mathbf{k}_\alpha \sigma}(t) = \epsilon_{\mathbf{k}_\alpha \sigma}^0 + q v_\alpha(t)$ is the energy levels in lead α where $\epsilon_{\mathbf{k}_\alpha \sigma}^0$ is the bare energy levels and $v_\alpha(t)$ is the applied external bias. The bias voltage is assumed to be $v_\alpha(t) = v_\alpha \theta(t)$ in order to study the transient dynamics of the system. H_N is the Hamiltonian of the nonmagnetic scattering region which reads

$$H_N = \sum_{n\sigma} \epsilon_n(t) d_{n\sigma}^\dagger d_{n\sigma}, \tag{4}$$

where $d_{n\sigma}^\dagger$ ($d_{n\sigma}$) and $\epsilon_n(t)$ is the creation (annihilation) operator of electrons and energy levels in the nonmagnetic system, respectively. H_T is the Hamiltonian describing the coupling between the magnetic electrodes and the nonmagnetic scattering region with the coupling constant $v_{\mathbf{k}_\alpha n}(t)$,

$$H_T = \sum_{\mathbf{k}_\alpha n\sigma} [v_{\mathbf{k}_\alpha n}(t) c_{\mathbf{k}_\alpha \sigma}^\dagger d_{n\sigma} + \text{H.c.}]. \tag{5}$$

To study the current-induced STT, the magnetic orientation of the left electrode is assumed to be pinned while that in the right lead is free to rotate. When the electrons in the left lead flow through the nonmagnetic scattering region and enter into the right lead, its magnetization direction rotates by an angle θ. This is due to the spin angular momentum difference between the incoming and outgoing spin-polarized electrons in the right electrode which generates a torque and exerts on the local moments of the right electrode. Such a torque describes the spin angular momentum transfer from the left lead to the

right lead by the spin polarized current. In our present work, we only consider the in-plane component of the current-induced STT since the in-plane STT component is much larger than the out-of-plane one in metallic spin valves as reported in the previous study [34]. The in-plane STT can be defined as [35–37]

$$\tau = \frac{i}{\hbar}\langle[H_T, S_R]\rangle,\tag{6}$$

where S_R is the total spin of the right lead along the x' direction since the STT should be along the direction of x' [35,38],

$$S_R = \frac{\hbar}{2}\sum_{\mathbf{k}_R\sigma}(c^{\dagger}_{\mathbf{k}_R\sigma}c_{\mathbf{k}_R\bar{\sigma}}\cos\theta - \sigma c^{\dagger}_{\mathbf{k}_R\sigma}c_{\mathbf{k}_R\sigma}\sin\theta).\tag{7}$$

Therefore, the STT operator can be expressed as

$$\tau(t) = -\sum_{\mathbf{k}_R n}\operatorname{Re}\operatorname{Tr}_{\sigma}[v_{\mathbf{k}_R n}(t)G^{<}_{n,\mathbf{k}_R}(t,t)\tilde{R}],\tag{8}$$

where

$$\tilde{R} = \begin{pmatrix}-\sin\theta & \cos\theta \\ \cos\theta & \sin\theta\end{pmatrix},\tag{9}$$

and the lesser Green function $G^{<}_{n,\mathbf{k}_R}(t,t)$ is defined in the spin space with $G^{<,\sigma\sigma'}_{n,\mathbf{k}_R}(t,t') \equiv i\langle c^{\dagger}_{\mathbf{k}_R\sigma'}(t')d_{n\sigma}(t)\rangle$.

Using the analytic continuation, the STT can be written as

$$\tau(t) = -\operatorname{Re}\operatorname{Tr}\int dt'\big[G^{r}(t,t')\Sigma^{<}_R(t',t) + G^{<}(t,t')\Sigma^{a}_R(t',t)\big]\tilde{R},\tag{10}$$

where $G^{r(<)}(t,t')$ is the retarded (lesser) Green's function of the scattering region in the spin space. Therefore, the current-induced STT under the dc bias can be expressed as

$$\tau = -\frac{1}{2}\int\frac{d\epsilon}{2\pi}(f_L - f_R)\operatorname{Tr}[G^{r}(\epsilon)\Gamma_L(\epsilon)G^{a}(\epsilon)\Gamma_R(\epsilon)\tilde{R}],\tag{11}$$

where $\Gamma_{\alpha}(\epsilon) = i[\Sigma^{r}_{\alpha}(\epsilon) - \Sigma^{a}_{\alpha}(\epsilon)]$ is the linewidth function.

Within the DFT framework, the current-induced STT in Eq. (10) can be rewritten as (see details in Appendix A)

$$\tau(t) = -\operatorname{Tr}\int dk_{\parallel}\big\{\bar{\Gamma}_R\big[\operatorname{Re}[H_{k_{\parallel},CC}(t)G^{<}_{k_{\parallel},CC}(t,t)]$$
$$-\frac{i}{2}\partial_t G^{<}_{k_{\parallel},CC}(t,t)\big]\bar{\Gamma}_R\big\}\bar{R}.\tag{12}$$

The lesser Green's function satisfies the Keldysh equation,

$$G^{<}_{k_{\parallel}}(t,t) = i\sum_{\alpha}\int\frac{d\epsilon}{2\pi}f(\epsilon)[A_{k_{\parallel}\alpha}(\epsilon,t)\Gamma_{\alpha}A^{\dagger}_{k_{\parallel}\alpha}(\epsilon,t)],\tag{13}$$

where the spectral function $A_{k_{\parallel}\alpha}(\epsilon,t)$ is defined as

$$A_{k_{\parallel}\alpha}(\epsilon,t) = \int_{-\infty}^{t}dt'e^{i\int_{t'}^{t}v_{\alpha}(\tau)d\tau}e^{i\epsilon(t-t')}G^{r}_{k_{\parallel}}(t,t').\tag{14}$$

For the upward pulse of bias, the analytic expression of $A_{k_{\parallel}\alpha}(\epsilon,t)$ can be obtained from Ref. [39]

$$A_{k_{\parallel}\alpha}(\epsilon,t) = \bar{G}^{r}_{k_{\parallel}}(\epsilon + v_{\alpha})$$
$$-\int\frac{d\omega}{2\pi i}\frac{e^{-i(\omega-\epsilon)t}\bar{G}^{r}_{k_{\parallel}}(\omega+v_{\alpha})}{\omega-\epsilon+v_{\alpha}-i0^{+}}\bigg[\frac{v_{\alpha}}{\omega-\epsilon-i0^{+}}$$
$$+\bigg(\Delta_{k_{\parallel}} - \sum_{\beta}v_{\beta}Y^{k_{\parallel}}_{\alpha\beta}(\epsilon,\omega)\bigg)\tilde{G}^{r}_{k_{\parallel}}(\epsilon)\bigg],\tag{15}$$

with

$$Y^{k_{\parallel}}_{\alpha\beta}(\epsilon,\omega) = \frac{\tilde{\Sigma}^{r}_{k_{\parallel}\beta}(\epsilon) - \tilde{\Sigma}^{r}_{k_{\parallel}\beta}(\omega+v_{\alpha}-v_{\beta})}{\epsilon-\omega-v_{\alpha}+v_{\beta}}.\tag{16}$$

Here $\tilde{G}^{r}(\omega) = [\omega I - \tilde{H}_{k_{\parallel}} - \tilde{\Sigma}^{r}_{k_{\parallel}}(\omega)]^{-1}$ and $\tilde{H}_{k_{\parallel}}$ are the equilibrium retarded Green's function and Hamiltonian, respectively, while $\bar{G}^{r}_{k_{\parallel}}(\omega) = [\omega I - \bar{H}_{k_{\parallel}} - \bar{\Sigma}^{r}_{k_{\parallel}}(\omega)]^{-1}$ and $\bar{H}_{k_{\parallel}}$ are the nonequilibrium Green's function and Hamiltonian, respectively. $\Delta_{k_{\parallel}} = \bar{H}_{k_{\parallel}} - \tilde{H}_{k_{\parallel}}$ is the change of internal potential landscape due to the external bias.

In order to calculate the time-dependent STT, one has to perform a double integral over energy [see Eqs. (13) and (15)] besides the integral over the k points in the Brillouin zone which makes the calculation extremely time consuming. In addition, the integral over energy is difficult to converge because many poles of the Green's function in the complex energy plane are close to the real energy axis and the integral over the k points is also hard to converge since there are always transmission spikes scattered around in the Brillouin zone for the layered system. Due to its successful application on the computation of time-dependent charge current and heat current [28,29], the CAP method has proven to be a powerful tool to study the time-dependent transport properties by transforming the infinite open system to be a closed system. After introducing the CAP to replace the Hamiltonian of leads, the retarded Green's function can be cast into a wide-band form so that the energy integral may be carried out analytically. Within the CAP formalism, we define the retarded Green's function as

$$G^{r\prime}(\epsilon) = \bigg(\epsilon I - H + i\sum_{\alpha}W'_{\alpha}\bigg)^{-1},\tag{17}$$

where W'_{α} is the CAP matrix (see details in Appendix B). Then the lesser Green's function can be rewritten as

$$G^{<\prime}_{k_{\parallel}}(t,t) = 2i\sum_{\alpha}\int\frac{d\epsilon}{2\pi}f(\epsilon)[A'_{k_{\parallel}\alpha}(\epsilon,t)W_{\alpha}A'^{\dagger}_{k_{\parallel}\alpha}(\epsilon,t)],\tag{18}$$

where for the upward steplike pulse [28]

$$A'_{k_{\parallel}\alpha}(\epsilon,t) = \sum_{n}\frac{|\psi_{nk_{\parallel}}\rangle\langle\phi_{nk_{\parallel}}|}{\epsilon+v_{\alpha}-\epsilon_{nk_{\parallel}}} + \sum_{n}\frac{e^{i(\epsilon+v_{\alpha}-\epsilon_{nk_{\parallel}})t}}{\epsilon-\epsilon_{nk_{\parallel}}}$$
$$\times|\psi_{nk_{\parallel}}\rangle\langle\phi_{nk_{\parallel}}|\bigg[\frac{v_{\alpha}}{\epsilon+v_{\alpha}-\epsilon_{nk_{\parallel}}} - \Delta_{k_{\parallel}}\tilde{G}^{r\prime}_{k_{\parallel}}(\epsilon)\bigg].\tag{19}$$

By expanding the retarded Green's function in terms of its eigenstates as

$$\bar{G}_{k_\parallel}^{r'}(\epsilon) = \sum_n \frac{|\psi_{nk_\parallel}\rangle\langle\phi_{nk_\parallel}|}{\epsilon - \epsilon_{nk_\parallel}}, \qquad (20)$$

the integration over energy of the spectrum function in Eq. (15) is analytically solved by the residue theorem since Eq. (16) can be set to zero within the CAP method [28].

Although the energy integral in the spectrum function $A'_{k_\parallel\alpha}(\epsilon,t)$ has been obtained analytically, one still has to compute the integration over energy involving the Fermi distribution function in Eq. (18). In order to further enhance the computational efficiency, the Padé approximation is then introduced in which the Fermi distribution function can be expanded using the $[N-1/N]$ scheme [31],

$$f_p(\epsilon) = \frac{1}{2} - \sum_{j=1}^N \left[\frac{\eta_j}{\beta\epsilon + i\xi_j} + \frac{\eta_j}{\beta\epsilon - i\xi_j} \right], \qquad (21)$$

where $\beta = 1/(k_B T)$ with the Boltzmann's constant k_B and temperature T. It is obvious that $\pm i\xi_j/\beta$ are the jth poles of the Padé spectrum decomposition in the upper and lower half plane, respectively. The accuracy of the Padé spectrum decomposition scheme can be improved by increasing the number of terms N in the expansion. In general, higher order Padé expansion is required for the Fermi distribution function at lower temperature. After employing the Padé approximation, the energy integral involving the Fermi function can be solved by the residue theorem as well. Therefore, the lesser Green's function for calculating the transient current-induced STT under an upward pulse of bias can be finally expressed as (see details in Appendix C)

$$G_{k_\parallel}^{<'}(t,t) = 2\sum_\alpha \sum_j \frac{\eta_j}{\beta} A'_{k_\parallel\alpha}\left(i\frac{\xi_j}{\beta},t\right) W_\alpha A_{k_\parallel\alpha}^{'\dagger}\left(i\frac{\xi_j}{\beta},t\right)$$

$$+ 2\sum_\alpha \sum_{mn} B_{mk_\parallel}\left[\chi_1 W_\alpha + \chi_2 W_\alpha C_1 \right.$$

$$\left. + \chi_3 C_2 W_\alpha C_3 - \sum_p \chi_4 \Delta_{k_\parallel} B_{pk_\parallel}^0 W_\alpha C_4 \right] B_{nk_\parallel}^\dagger,$$

$$(22)$$

with

$$B_{mk_\parallel} = |\psi_{mk_\parallel}\rangle\langle\phi_{mk_\parallel}|, \qquad (23)$$

$$B_{pk_\parallel}^0 = |\psi_{pk_\parallel}^0\rangle\langle\phi_{pk_\parallel}^0|. \qquad (24)$$

Here, the following relation was used to expand the equilibrium Green's function $\tilde{G}^r(\epsilon)$:

$$\tilde{G}_{k_\parallel}^{r'}(\epsilon) = \sum_n \frac{|\psi_{nk_\parallel}^0\rangle\langle\phi_{nk_\parallel}^0|}{\epsilon - \epsilon_{nk_\parallel}^0}. \qquad (25)$$

To summarize, the following steps should be used in NEGF-DFT-CAP approach in calculating the transient behavior of STT under an upward pulse of bias. First of all, the traditional NEGF-DFT calculation should be performed to obtain the equilibrium (initial state) and nonequilibrium dc state (long time limit dc state) with enough k points. The CAP is then introduced to replace the Hamiltonian of lead. The transmission coefficient calculated from the exact NEGF-DFT formalism and the CAP method should be compared to make sure that the CAP region is long enough. Moreover, the Padé approximation of the Fermi function should be compared with the exact Fermi distribution function and the accuracy can be improved by increasing the expansion order of the Padé spectrum decomposition. Once the accuracy of both CAP method and Padé approximation are checked, the lesser Green's function of each k point can be numerically calculated from Eq. (22) and finally the time-dependent STT can be obtained from Eq. (12). In addition, in the final expression of transient STT, the energy integral can be evaluated by the residue theorem and the summation over the k points in the Brillouin zone is performed at the end. This approach significantly enhances the computational speed.

III. NUMERICAL RESULTS

In this section, the time-dependent current-induced STT due to an upward pulse is calculated numerically using the NEGF-DFT-CAP formalism for the Co/Cu/Co trilayer system. The two-probe system consists of two semi-infinite Co leads and a scattering region of five atomic Cu layers, as shown in Fig. 2. Both Co and Cu used here are in the fcc phase with the lattice constant of 3.54 Å and there are two atomic layers in one unit cell of the Co electrode. The first-principles transport calculation is implemented in the NEGF-DFT quantum transport package NANODCAL [40]. The local density approximation (LDA) by Ceperley and Alder [41] is employed for the exchange and correlation potential and the nonlocal norm-conserving pseudopotential is used for the core electrons [42]. The single-ζ polarized orbital basis is used for both Co and Cu atoms. The energy cutoff of the real space grid is taken as 4000 eV and the convergence criteria of the Hamiltonian and density matrix is set to be
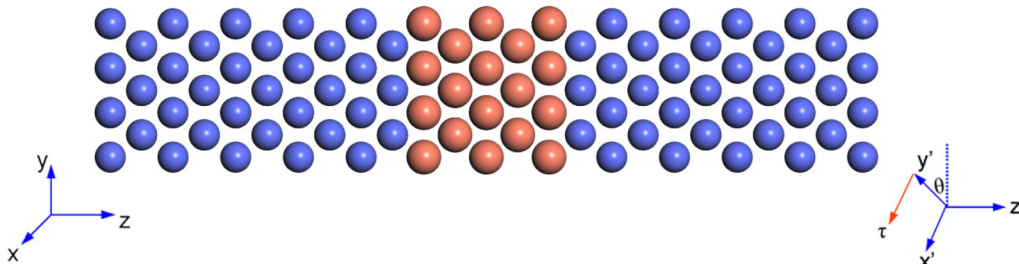

FIG. 2. Schematic diagram of the Co/Cu/Co trilayers. The blue and orange balls represent the cobalt and copper atoms, respectively.
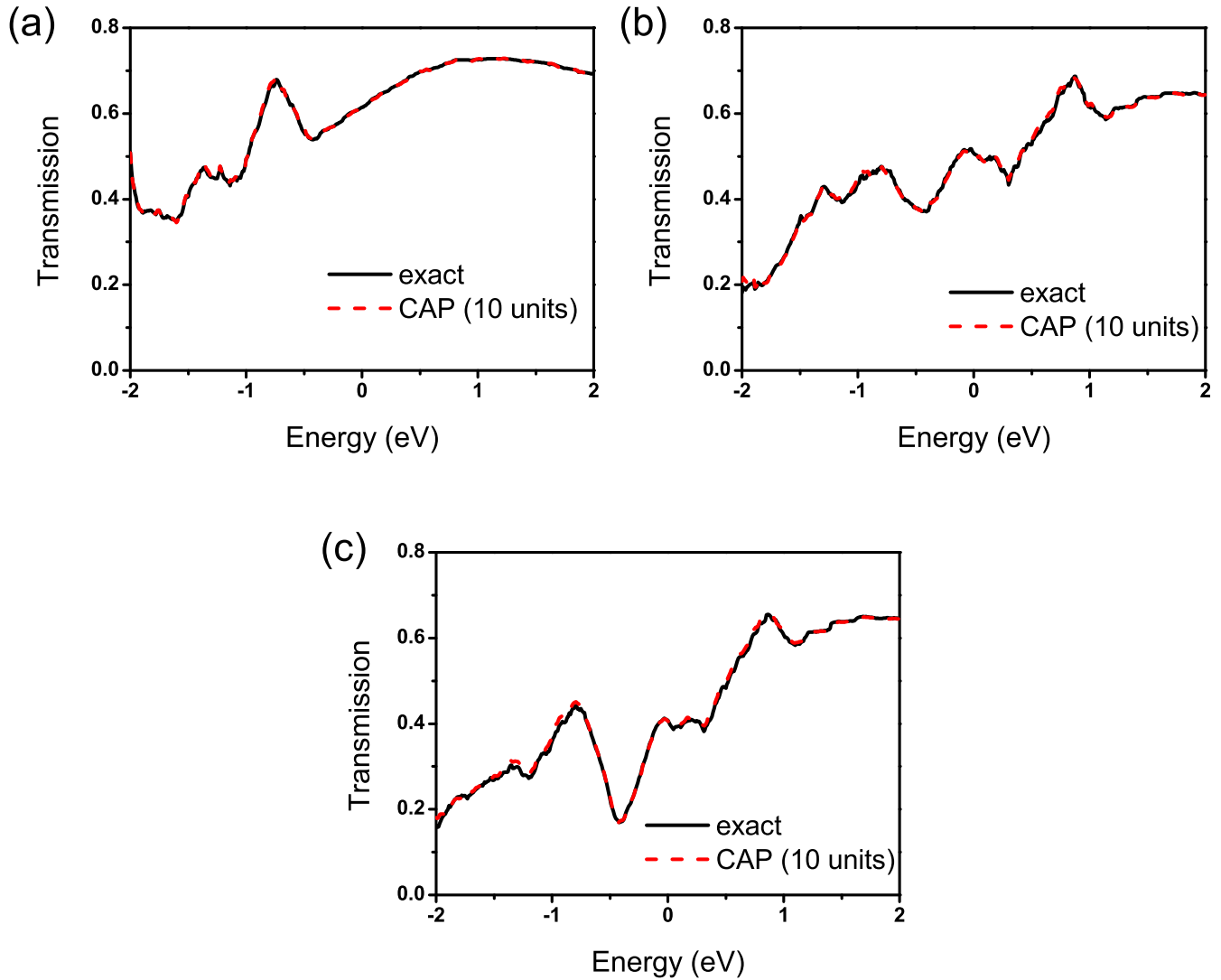
FIG. 3. Average transmission coefficients for (a) spin-up and (b) spin-down electrons in the P configurations and for (c) electrons of either spin in the AP configurations of the Co/Cu/Co trilayers calculated by exact method (black solid line) and CAP method (red dash line).

10^{-5} eV. The temperature in the Fermi distribution function in the calculation is set to 300 K. In the self-consistent calculation, a $30 \times 30 \times 1$ k mesh is sampled within the Brillouin zone which is sufficient for the convergence of Hamiltonian and density matrix. In order to calculate the transmission coefficients of the Co/Cu/Co system, a 80×80 k mesh is used. It is found that when a denser k grid is used, the difference in the transmission coefficients is less than 1%. In order to simplify the simulation for the system with different rotating angles of magnetization orientation, we only perform the DFT calculations with the collinear spin and then rigidly rotate magnetization in the right lead which is similar to the previous studies [43].

The GMR ratio is defined in terms of the conductances for spin-up and spin-down electrons in the parallel (P) and antiparallel (AP) configurations of the magnetic layers by

$$\text{GMR} = \frac{G_P^\uparrow + G_P^\downarrow - 2G_{AP}^{\uparrow,\downarrow}}{2G_{AP}^{\uparrow,\downarrow}} \times 100\%, \qquad (26)$$

where G_P^σ and G_{AP}^σ is the conductance of electrons with a given spin σ in the P and AP configurations, respectively. In the Co/Cu/Co system shown in Fig. 2, due to the symmetric structure, the conductances of the spin-up and spin-down electrons of the AP configuration should be the same. From the calculated conductance of the P and AP configurations, a GMR ratio of 38% is obtained for the proposed Co/Cu/Co trilayers under zero bias, which is consistent with previous calculations of similar systems [44,45].

In order to study the current-induced STT within the NEGF-DFT-CAP framework, the semi-infinite Co electrodes are replaced by CAP and three unit cells are used for the buffer region between the CAP region and the Cu layers. In order to reduce the reflection due to CAP region, 10 unit cells of Co electrodes with about 35.44 Å long in the transport direction is used to construct the CAP region for each lead. The comparison for the average transmission coefficients in the $k_\parallel$ space of Co/Cu/Co system calculated by the exact NEGF-DFT method and the CAP method is presented in Fig. 3. The transmission coefficient of the spin-up and spin-down
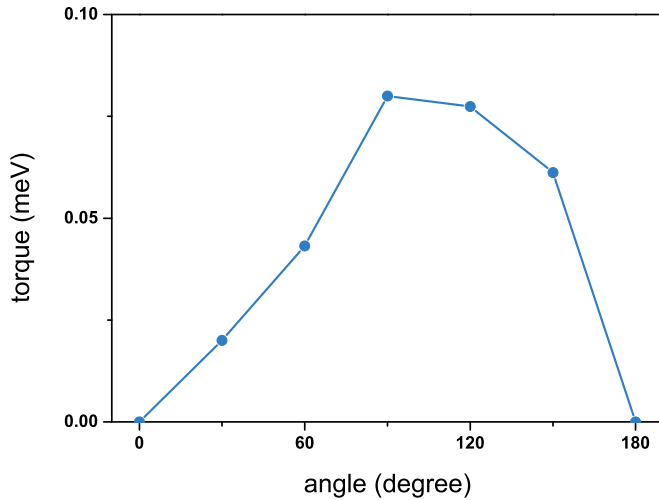
FIG. 4. Current-induced STT of Co/Cu/Co trilayers as a function of rotating angle θ of magnetization direction in the right lead under a dc bias of 10 mV.

electrons is about 0.62 and 0.51 at the Fermi level in the P configuration, as shown in Figs. 3(a) and 3(b), respectively. The spin polarization of the conductance defined as $\frac{G^\uparrow - G^\downarrow}{G^\downarrow}$ is about 22%, showing that the electron with majority spin dominates the transport through the Co/Cu/Co system in the P configuration. For the AP configuration, the transmission coefficient of either spin orientation is about 0.41 at the Fermi level, as plotted in Fig. 3(c), exhibiting the lowest transmission coefficient due to the large band mismatch of Co and Cu with different spins.

Moreover, it can be seen from Fig. 3 that the transmission coefficients calculated from the NEGF-DFT-CAP frame agree remarkably well with those obtained from the exact method. Therefore, the CAP region with the length of 10 unit cells of Co electrodes is long enough to accurately describe the transport properties of the Co/Cu/Co system in both P and AP configurations.

Figure 4 shows the current-induced STT of the Co/Cu/Co system under a dc bias of 10 mV with different rotating angles θ of magnetization orientation in the right lead calculated from Eq. (11). The maximum value of the current-induced STTs is around 0.08 meV which corresponds to about 3×10^{-17} J/A. This is similar to that obtained by the first-principles calculation in Ref. [24]. For $\theta = 0$, the system is symmetric and the self-energy with each spin is the same for left and right leads, i.e., $\Sigma^r_{L\sigma} = \Sigma^r_{R\sigma}$, while for $\theta = \pi$, the system is antisymmetric and one has $\Sigma^r_{L\sigma} = \Sigma^r_{R\bar{\sigma}}$. The Green's functions for these cases are diagonal in spin space so that the spin current is conserved and the current-induced STT is zero. It is found that the angular dependent STTs do not have the sinusoidal behavior which agrees with the previous theoretical studies [24,44].

We now examine the time-dependent current and current-induced STT induced by an upward pulse of external bias applied on the Co/Cu/Co system. Figure 5 presents the transient current $I_\sigma(t)$ of Co/Cu/Co trilayers with P and AP configurations under the upward pulse bias of 10 mV and 20 mV. We see that once the pulse bias is turned on, the transient currents decrease rapidly to the minimum value first

for the P configuration, while for the AP configuration the transient currents increase rapidly reaching the maximum first and decay with oscillations to the steady states. For the system under an upward pulse of 10 mV, the turn-on time to reach the minimum is about 20 fs and 40 fs for the spin-up and spin-down currents in the P configuration, respectively, as shown in Fig. 5(a). The transient currents then increase to the maximum value at about 120 fs, while for the AP configuration under a 10 mV upward pulse bias, the turn-on time is about 25 fs for both majority and minority spin currents and decreases to the minimum at about 180 fs, as shown in Fig. 5(c). In order to quantitatively study the relaxation time of the transient current to reach the steady state, the relaxation time τ_r is defined as $\kappa = 10\%$, where $\kappa = \frac{|I_\sigma(\tau_t) - I^{dc}_\sigma|}{I^{dc}_\sigma}$ with I^{dc}_σ being the dc limit of the spin-polarized transient current [47]. The relaxation time can reach 1190 fs for the spin-up current and only 600 fs for the spin-down current in the P configuration, while the relaxation time is about 760 fs and 520 fs for the majority and minority currents in the AP configuration, respectively.

When the applied pulse bias increases to 20 mV, it is found that the spin-polarized transient current shows less peaks once the bias is turned on for both P and AP configurations, as shown in Figs. 5(b) and 5(d), respectively. The oscillation frequency of the transient current is found to be proportional to the applied bias v_α, which agrees with previous studies [46,47]. This is because the oscillation of the transient current is dominated by the oscillatory term $e^{i(\epsilon + v_\alpha - \epsilon_{nk})t}$ in the spectrum function $A'_{k_\parallel \alpha}(\epsilon, t)$ in Eq. (19). For instance, the period between two adjacent peaks is about 170 fs and 310 fs for the spin-up current in the P configuration under the pulse bias of 10 mV and 20 mV, as shown in Figs. 5(a) and 5(b), respectively.

The transient STT with different rotating angles θ of magnetization direction in the right lead obtained from the NEGF-DFT-CAP framework is plotted in Fig. 6. It is found that the time-dependent STTs of the Co/Cu/Co system show almost the same profile for different rotating angles of $\theta = \frac{\pi}{6}$, $\frac{\pi}{3}$, and $\frac{\pi}{2}$ in the right lead. This is because we only perform a collinear DFT calculation and the magnetization directions are simply introduced in the right lead. Therefore, the resonant states in the central region of the Co/Cu/Co system are roughly the same for different rotating angles which leads to the same oscillating profile of the time-dependent STTs, since it is the resonant state that is responsible for the oscillation. Once the upward pulse of bias is switched on, the current-induced STTs dramatically increase to a large positive value. The transient STTs reach the maximum value after about 165 fs and then start to decay with oscillation. After about 560 fs, the transient STTs change their signs to negative and arrive at the minimum value at about 750 fs. The STTs then increase to approach oscillatory quasisteady states with a long relaxation time of approximately 7500 fs (not shown in Fig. 6). It is found that the transient STTs show the oscillation in a damped fashion after about 1500 fs with almost the same period about 100 fs which mainly originate from the oscillation of the transient spin-up current as shown in the inset of Fig. 6. In addition, for the Co/Cu/Co system the larger the rotating angle θ, the larger the absolute value of the transient STT is (as long
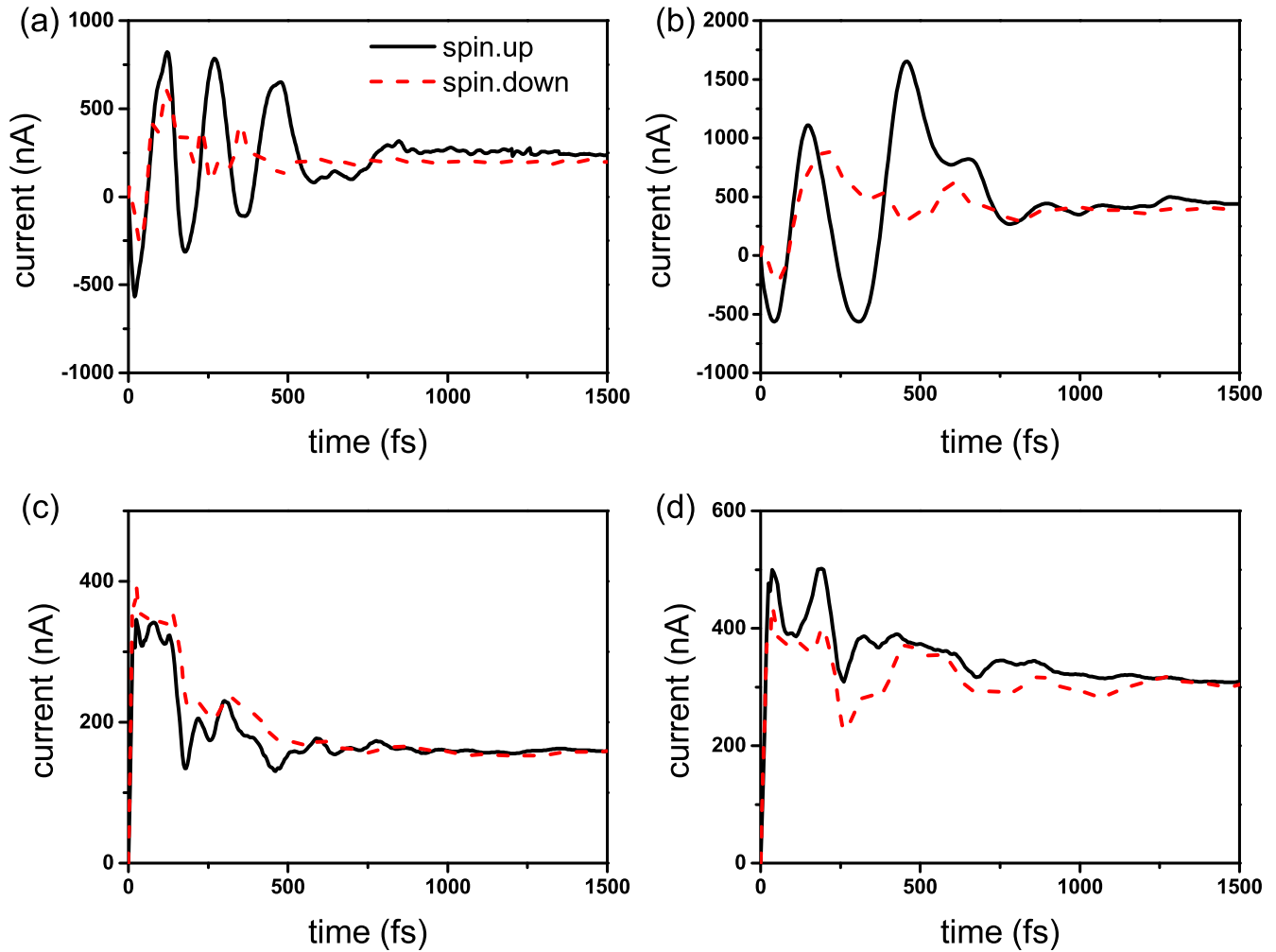
FIG. 5. Transient spin-polarized current of Co/Cu/Co trilayers with P configuration under an upward pulse bias of (a) 10 mV and (b) 20 mV, and with AP configuration under an upward pulse bias of (c) 10 mV and (d) 20 mV. The black solid curves and red dash curves indicate the spin-up and spin-down transient current, respectively.
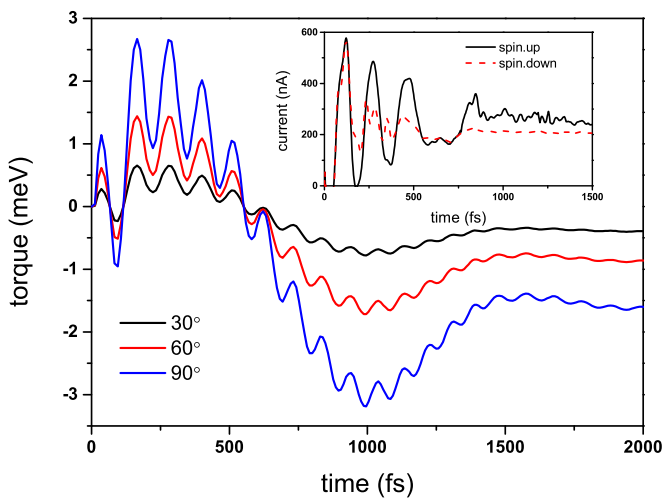

FIG. 6. Transient current-induced STT of Co/Cu/Co trilayers under an upward pulse bias of 10 mV with different θ. Inset: transient spin-polarized current for the system with $\theta = 30°$.

as $\theta < \frac{\pi}{2}$). We note that the oscillatory behavior of STT in the long time is reminiscent of resonance in typical transient behavior.

To understand this oscillation behavior of the time-dependent STT, we take the Fourier transform of the transient spin-up current with the rotating angle $\theta = 30°$ under a pulse bias of 10 mV to study the resonant states which contribute to the oscillation of time-dependent current-induced STT, as shown in Fig. 7. The Fourier transformed current shows several considerable peaks at low frequency, especially an intense peak at $\omega = 50$ meV. We now examine the transient spin-up current contributed by the energy of 50 meV. The upper panel of inset in Fig. 7 presents the time-dependent spin-up current for the energy of 50 meV at the Γ point. We find that it contributes significantly to the oscillation of total spin-up current and further to the transient STT. This oscillation can be explained by the corresponding scattering states of the Co/Cu/Co trilayers shown in the lower panel of the inset in Fig. 7. The real-space scattering states are mainly localized on the Co atom at the Co/Cu interface. Such interface resonant
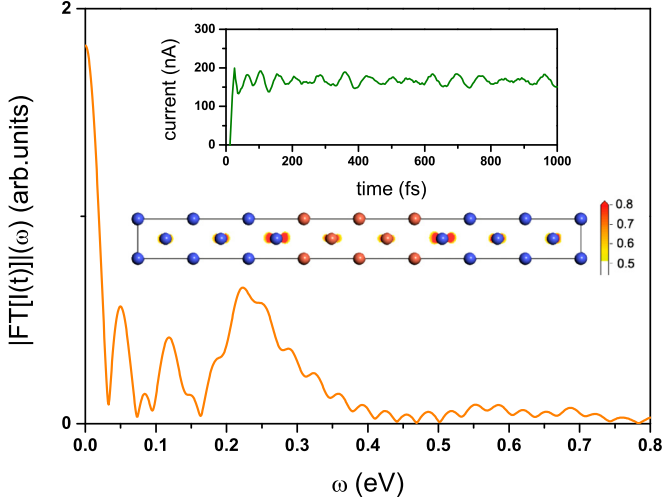
FIG. 7. Fourier transform of transient spin-up current for the Co/Cu/Co trilayers with $\theta = 30°$ under an upper pulse bias of 10 mV. Inset: corresponding transient spin-up current (upper panel) and real-space distribution of scattering states (lower panel) with the energy of 50 meV at the Γ point.

states give rise to the continuous oscillation of transient STT.

IV. CONCLUSION

Based on the NEGF-DFT-CAP framework, the time-dependent current-induced STT under an upward pulse of bias voltage was studied for the layered magnetic systems. To reduce the computational complexity, we employed the technique of CAP and cast the lesser Green's function into a wide-band form making analytic calculation possible. In order to further speed up the calculation, the Padé approximation is introduced to replace the Fermi distribution function. As such all energy integrals in the formalism of transient STT can be solved by the residue theorem, which significantly reduces the computational complexity. The NEGF-DFT-CAP formalism with the Padé approximation is then implemented to study the transient current and transient current-induced STT of the Co/Cu/Co trilayers under an upward pulse of bias with different rotating angle of magnetization direction between two leads. We find the spin-polarized transient current shows a damped oscillatory behavior with the oscillation frequency proportional to the applied bias. The time-dependent STTs show similar profile for systems with different rotating angles. Moreover, a persistent oscillation is obtained for the transient STT when it approaches the steady state in the long-time limit originated from the interface resonant state.

APPENDIX A: STT FORMALISM WITHIN THE DFT FRAMEWORK

Within the DFT framework, the whole time-dependent Hamiltonian can be expressed as

$$\begin{bmatrix} H_{LL}(t) & H_{LC}(t) & 0 \\ H_{CL}(t) & H_{CC}(t) & H_{CR}(t) \\ 0 & H_{RC}(t) & H_{RR}(t) \end{bmatrix}. \tag{A1}$$

Here, all submatrices $H_{\alpha\beta}$ are 2×2 block matrices in spin space. Note that we have to use the orthogonal basis set to expand the Hamiltonian in the time-dependent transport calculation from first principles [28]. For the lesser Green's function projected on the central scattering region, we find [28,48]

$$i\frac{\partial}{\partial t} G_{CC}^<(t,t') = H_{CC}(t) G_{CC}^<(t,t')$$
$$+ \int_0^t \left[\Sigma^<(t,t_1) G_{CC}^a(t_1,t') + \Sigma^r(t,t_1) G_{CC}^<(t_1,t') \right] dt_1 \tag{A2}$$

and

$$-i\frac{\partial}{\partial t'} G_{CC}^<(t,t') = G_{CC}^<(t,t') H_{CC}(t')$$
$$+ \int_0^t \left[G_{CC}^r(t,t_1) \Sigma^<(t_1,t') + G_{CC}^<(t,t_1) \Sigma^a(t_1,t') \right] dt_1. \tag{A3}$$

After subtracting Eq. (A3) by Eq. (A2) and setting $t = t'$, one can obtain

$$\text{Re} \int_0^t \left[G_{CC}^r(t,t_1) \Sigma^<(t_1,t') + G_{CC}^<(t,t_1) \Sigma^a(t_1,t') \right] dt_1$$
$$= \text{Re}[H_{CC}(t) G_{CC}^<(t,t)] - \frac{i}{2} \frac{\partial}{\partial t} G_{CC}^<(t,t). \tag{A4}$$

By introducing a projection matrix

$$\bar{\Gamma}_R = \begin{bmatrix} 0 & 0 & 0 \\ 0 & 0 & 0 \\ 0 & 0 & I_R \end{bmatrix}, \tag{A5}$$

where I_R is the unit matrix with the same dimension as the linewidth function of the right lead, the self-energy of the right lead can be written as

$$\Sigma_R^\gamma(t,t') = \bar{\Gamma}_R \Sigma^\gamma(t,t') \bar{\Gamma}_R, \tag{A6}$$

with $\gamma = r,a,<$. If the layered structure is considered, the k sampling is needed in the x-y plane since the system is periodical in the x and y direction. Substituting Eq. (A4) into Eq. (10), the current-induced STT can be written as

$$\tau(t) = -\text{Tr} \int dk_\parallel \left\{ \bar{\Gamma}_R \left[\text{Re}[H_{k_\parallel,CC}(t) G_{k_\parallel,CC}^<(t,t)] \right. \right.$$
$$\left. \left. - \frac{i}{2} \partial_t G_{k_\parallel,CC}^<(t,t) \right] \bar{\Gamma}_R \right\} \bar{R}. \tag{A7}$$

Here $\bar{R} = \tilde{R} \otimes I_C$, where I_C is the unit matrix with the same dimension as the Hamiltonian of the central region.

APPENDIX B: COMPLEX ABSORBING POTENTIAL IN THE GREEN'S FUNCTION

Within the NEGF-CAP framework, we use W'_α instead of the self-energy in the retarded Green's function in Eq. (17) where $W'_L = \begin{pmatrix} W_L & 0 & 0 \\ 0 & 0 & 0 \\ 0 & 0 & 0 \end{pmatrix}$, $W'_R = \begin{pmatrix} 0 & 0 & 0 \\ 0 & 0 & 0 \\ 0 & 0 & W_R \end{pmatrix}$, and W_α is the CAP to replace the α lead. In the first-principles approach with linear combination of atomic orbitals (LCAO) basis, W should be calculated in the orbital space [28],

$$W_{\mu\nu} = \int d\mathbf{r}\, \zeta^*_\mu(\mathbf{r}) W(z) \zeta_\nu(\mathbf{r}), \tag{B1}$$

where $\zeta_{\mu(\nu)}$ is the atomic basis set and $W(z)$ is defined in the real space [49,50],

$$W(z) = \frac{\hbar^2}{2m}\left(\frac{2\pi}{\Delta z}\right)^2 f(z), \tag{B2}$$

with

$$f(z) = \frac{4}{c^2}\left[\left(\frac{\Delta z}{z_2 - 2z_1 + z}\right)^2 + \left(\frac{\Delta z}{z_2 - z}\right)^2 - 2\right]. \tag{B3}$$

Here $\Delta z = z_2 - z_1$ is the length of the CAP region with z_1 and z_2 the starting and ending points of the CAP region of each lead along the transport direction z, respectively. c is set to be 2.62 as a constant.

APPENDIX C: DEFINITIONS OF χ_n AND C_n

In the final expression of $G^{<\prime}_{k_\parallel}(t,t)$ in Eq. (22), the notations of χ_n and C_n are defined as follows:

$$\chi_1 = \frac{f_p(\epsilon_{mk_\parallel} - v_\alpha)}{\epsilon_{mk_\parallel} - \epsilon^*_{nk_\parallel}}, \tag{C1}$$

$$\chi_2 = f_p(\epsilon^*_{nk_\parallel} - v_\alpha)\frac{e^{i(\epsilon^*_{nk_\parallel} - \epsilon_{mk_\parallel})t}}{\epsilon_{mk_\parallel} - \epsilon^*_{nk_\parallel} + v_\alpha}, \tag{C2}$$

$$\chi_3 = f_p(\epsilon_{mk_\parallel})\frac{e^{i(\epsilon_{mk_\parallel} - \epsilon_{nk_\parallel})t}}{\epsilon_{mk_\parallel} - \epsilon^*_{nk_\parallel}}, \tag{C3}$$

$$\chi_4 = \frac{f(\epsilon^0_{pk_\parallel})}{(\epsilon^0_{pk_\parallel} - \epsilon_{mk_\parallel})(\epsilon^0_{pk_\parallel} - \epsilon^*_{nk_\parallel})} \tag{C4}$$

and

$$C_1 = \frac{v_\alpha}{\epsilon^*_{nk_\parallel} - \epsilon_{mk_\parallel}} - \Delta_{k_\parallel}\tilde{G}^{r\prime}_{k_\parallel}(\epsilon^*_{nk_\parallel} - v_\alpha), \tag{C5}$$

$$C_2 = I - \Delta_{k_\parallel}\tilde{G}^{r\prime}_{k_\parallel}(\epsilon_{mk_\parallel}), \tag{C6}$$

$$C_3 = \frac{v_\alpha}{\epsilon_{mk_\parallel} - \epsilon^*_{nk_\parallel} + v_\alpha} - \tilde{G}^{a\prime}_{k_\parallel}(\epsilon_{mk_\parallel})\Delta_{k_\parallel}, \tag{C7}$$

$$C_4 = \frac{v_\alpha}{\epsilon^0_{pk_\parallel} - \epsilon^*_{nk_\parallel} + v_\alpha} - \tilde{G}^{a\prime}_{k_\parallel}(\epsilon^0_{pk_\parallel})\Delta_{k_\parallel}. \tag{C8}$$

[1] G. A. Prinz, Science **282**, 1660 (1998).

[2] S. A. Wolf, D. D. Awschalom, R. A. Buhrman, J. M. Daughton, S. von Molnar, M. L. Roukes, A. Y. Chtchelkanova, and D. M. Treger, Science **294**, 1488 (2001).

[3] M. N. Baibich, J. M. Broto, A. Fert, F. N. Van Dau, F. Petroff, P. Etienne, G. Creuzet, A. Friederich, and J. Chazelas, Phys. Rev. Lett. **61**, 2472 (1988).

[4] G. Binasch, P. Grünberg, F. Saurenbach, and W. Zinn, Phys. Rev. B **39**, 4828(R) (1989).

[5] J. S. Moodera, L. R. Kinder, T. M. Wong, and R. Meservey, Phys. Rev. Lett. **74**, 3273 (1995).

[6] T. Miyazaki and N. Tezuka, J. Magn. Magn. Mater. **151**, 403 (1995).

[7] J. C. Slonczewski, J. Magn. Magn. Mater. **159**, L1 (1996).

[8] L. Berger, J. Appl. Phys. **55**, 1954 (1984).

[9] L. Berger, Phys. Rev. B **54**, 9353 (1996).

[10] M. Tsoi, A. G. M. Jansen, J. Bass, W.-C. Chiang, M. Seck, V. Tsoi, and P. Wyder, Phys. Rev. Lett. **80**, 4281 (1998).

[11] J. A. Katine, F. J. Albert, R. A. Buhrman, E. B. Myers, and D. C. Ralph, Phys. Rev. Lett. **84**, 3149 (2000).

[12] J. Grollier, V. Cros, A. Hamzic, J. M. George, H. Jaffrès, A. Fert, G. Faini, J. B. Youssef, and H. Legall, Appl. Phys. Lett. **78**, 3663 (2001).

[13] X. Waintal, E. B. Myers, P. W. Brouwer, and D. C. Ralph, Phys. Rev. B **62**, 12317 (2000).

[14] C. Heide, P. E. Zilberman, and R. J. Elliott, Phys. Rev. B **63**, 064424 (2001).

[15] C. Heide, Phys. Rev. Lett. **87**, 197201 (2001).

[16] S. Zhang, P. M. Levy, and A. Fert, Phys. Rev. Lett. **88**, 236601 (2002).

[17] Z. Li and S. Zhang, Phys. Rev. B **68**, 024404 (2003).

[18] Z. Li and S. Zhang, Phys. Rev. Lett. **92**, 207203 (2004).

[19] D. Waldron, V. Timoshevskii, Y. Hu, K. Xia, and H. Guo, Phys. Rev. Lett. **97**, 226802 (2006).

[20] D. Waldron, L. Liu, and H. Guo, Nanotechnology **18**, 424026 (2007).

[21] P. M. Haney, D. Waldron, R. A. Duine, A. S. Núñez, H. Guo, and A. H. MacDonald, Phys. Rev. B **75**, 174428 (2007).

[22] Y. Ke, K. Xia, and H. Guo, Phys. Rev. Lett. **100**, 166805 (2008).

[23] K. Gong, L. Zhang, L. Liu, Y. Zhu, G. Yu, P. Grutter, and H. Guo, J. Appl. Phys **118**, 093902 (2016).

[24] S. Wang, Y. Xu, and K. Xia, Phys. Rev. B **77**, 184430 (2008).

[25] X. Jia, K. Xia, Y. Ke, and H. Guo, Phys. Rev. B **84**, 014401 (2011).

[26] D. Liu, X. Han, and H. Guo, Phys. Rev. B **85**, 245436 (2012).

[27] V. Timoshevskii, Y. Hu, E. Marcotte, and H. Guo, J. Phys.: Condens. Matter **26**, 015002 (2014).

[28] L. Zhang, J. Chen, and J. Wang, Phys. Rev. B **87**, 205401 (2013).

[29] Z. Yu, L. Zhang, Y. Xing, and J. Wang, Phys. Rev. B **90**, 115428 (2014).

[30] J. Hu, R.-X. Xu, and Y. Yan, J. Chem. Phys. **133**, 101106 (2010).

[31] J. Hu, M. Luo, F. Jiang, R.-X. Xu, and Y. Yan, J. Chem. Phys. **134**, 244106 (2011).

[32] H. Xie, Y. Kwok, Y. Zhang, F. Jiang, X. Zheng, Y. Yan, and G. Chen, Phys. Status Solidi B **250**, 2481 (2013).

[33] K. T. Cheung, B. Fu, Z. Yu, and J. Wang, Phys. Rev. B **95**, 125422 (2017).

[34] A. Brataas, G. E. W. Bauer, and P. J. Kelly, Phys. Rep. **427**, 157 (2006).

[35] Z.-G. Zhu, G. Su, Q.-R. Zheng, and B. Jin, Phys. Rev. B **68**, 224413 (2003).

[36] Z.-G. Zhu, G. Su, B. Jin, and Q.-R. Zheng, Phys. Lett. A **306**, 249 (2003).

[37] Y. Yu, H. Zhan, L. Wan, B. Wang, Y. Wei, Q. Sun, and J. Wang, Nanotechnology **24**, 155202 (2013).

[38] G.-M. Tang and J. Wang, Phys. Rev. B **90**, 195422 (2014).

[39] J. Maciejko, J. Wang, and H. Guo, Phys. Rev. B **74**, 085324 (2006).

[40] J. Taylor, H. Guo, and J. Wang, Phys. Rev. B **63**, 245407 (2001).

[41] D. M. Ceperley and B. J. Alder, Phys. Rev. Lett. **45**, 566 (1980).

[42] N. Troullier and J. L. Martins, Phys. Rev. B **43**, 1993 (1991).

[43] C. Heiliger and M. D. Stiles, Phys. Rev. Lett. **100**, 186805 (2008).

[44] P. M. Haney, D. Waldron, R. A. Duine, A. S. Núñez, H. Guo, and A. H. MacDonald, Phys. Rev. B **76**, 024404 (2007).

[45] J. Mathon, A. Umerski, and M. Villeret, Phys. Rev. B **55**, 14378 (1997).

[46] B. Wang, Y. Xing, L. Zhang, and J. Wang, Phys. Rev. B **81**, 121103(R) (2010).

[47] B. Wang, J. Li, F. Xu, Y. Wei, J. Wang, and H. Guo, Nanoscale **7**, 10030 (2015).

[48] H. Haug and A.-P. Jauho, *Quantum Kinetics in Transport and Optics of Semiconductors* (Springer-Verlag, Berlin, 1998).

[49] D. E. Manolopoulos, J. Chem. Phys. **117**, 9552 (2002).

[50] J. A. Driscoll and K. Varga, Phys. Rev. B **78**, 245118 (2008).